



Research Article

Role of Activated Carbon from Arabica Coffee Waste in Enhancing the Dehydrogenation Properties of Magnesium Hydride (MgH₂) for Hydrogen Storage

Adi Setiawan*

Mechanical Engineering Department, Faculty of Engineering, Universitas Malikussaleh, Jalan Batam, Bukit Indah, Lhokseumawe, Indonesia

Zulkarnain Jalil*

Department of Physics, Faculty of Mathematics and Natural Sciences, Syiah Kuala University, Banda Aceh, Indonesia

Siti Nurjannah and Shafira Riskina

Magister Program in Renewable Energy Engineering, Faculty of Engineering, Universitas Malikussaleh, Jalan Batam, Bukit Indah, Lhokseumawe, Indonesia

Muhammad Muhammad

Chemical Engineering Department, Faculty of Engineering, Universitas Malikussaleh, Jalan Batam, Bukit Indah, Lhokseumawe, Indonesia

* Corresponding author. E-mail: adis@unimal.ac.id; zjalil@usk.ac.id DOI: 10.14416/j.asep.2025.05.010

Received: 4 December 2024; Revised: 27 January 2025; Accepted: 6 March 2025; Published online: 30 May 2025
© 2025 King Mongkut's University of Technology North Bangkok. All Rights Reserved.

Abstract

Solid-state hydrogen storage requires improvement through catalyst-added methods to maximize performance. Magnesium Hydride (MgH₂) is a type of solid-state hydrogen storage that is highly developed today but has many shortcomings, including high dehydrogenation temperatures. The use of carbon-based catalysts derived from biomass offers dual advantages by harnessing agricultural waste and supporting environmentally sustainable practices. This study utilized activated carbon (AC) from Arabica coffee agroindustry waste, specifically from pulp and parchment, as a catalyst to enhance the properties of MgH₂. The activated carbons from coffee pulp and parchment (ACs) were produced through slow pyrolysis at 400 °C and chemically activated using potassium hydroxide (KOH) and sodium hydroxide (NaOH) solutions at various concentrations. Composites of MgH₂ + 5 wt% AC were prepared through three hours of intensive mechanical alloying. Initially, the ACs were characterized using iodine adsorption, FTIR, TGA-DSC, and SEM analyses. The MgH₂ + 5 wt% AC composites were then subjected to characterization through XRD, TGA-DTA, and SEM analysis. The results of the thermal investigations indicated that the AC catalysts from coffee pulp and parchment significantly reduced the onset temperature of dehydrogenation for MgH₂. The lowest dehydrogenation temperature was 342.36 °C, achieved by adding 5 wt% AC produced from coffee parchment that was chemically activated using a 2% KOH solutions.

Keywords: Activated carbon, Catalyst, Coffee waste, Magnesium hydride, Solid hydrogen storage

1 Introduction

The global transition towards cleaner and renewable energy sources has sparked significant interest in

hydrogen as a sustainable alternative to traditional fossil fuels. Hydrogen is particularly attractive due to its impressive energy density, standing at 142 MJ/kg,



which allows for efficient energy storage and transfer [1], [2]. Additionally, the combustion of hydrogen produces only water vapor as a byproduct, thus making it environmentally benign and contributing to the reduction of greenhouse gas emissions. Despite these advantages, hydrogen storage remains a formidable challenge.

A significant challenge lies in hydrogen's low volumetric energy density, which results in substantial volume requirements relative to its energy content. This characteristic complicates the development of efficient storage solutions. Furthermore, under ambient conditions, hydrogen is highly volatile and can easily escape from containment systems, raising safety concerns and making storage and transportation both difficult and expensive [3]. As the demand for sustainable energy solutions continues to grow, overcoming these storage challenges will be crucial for enabling the wider adoption of hydrogen in future energy systems.

Several methods have been developed to address the challenges associated with hydrogen storage, including high-pressure storage, cryogenic storage, and chemical hydrogen storage [4]–[7]. Among these options, solid-state hydrogen storage stands out as particularly promising due to its inherent safety, compactness, and higher storage capacity at moderate temperatures and pressures. Notably, magnesium hydride (MgH_2) is a metal hydride with a high hydrogen content of approximately 7.6 wt%, making it a suitable candidate for solid-state hydrogen storage [8]. Previous research has found that nanocrystalline materials of MgH_2 -Ti had a hydrogen storage capacity of 2.7 wt% [9]. However, the practical use of MgH_2 is limited by its high dehydrogenation temperature and slow kinetics for hydrogen adsorption and desorption. These limitations primarily arise from the high dissociation enthalpy and sluggish reaction kinetics of MgH_2 , which hinder its effectiveness in real-world applications.

One promising strategy to enhance the hydrogen storage performance of MgH_2 is the incorporation of catalysts. These catalysts play a crucial role in reducing the activation energy required for hydrogen release, thereby enhancing the dehydrogenation kinetics. As a result, hydrogen can be desorbed at much lower temperatures, significantly improving the process efficiency.

Aceh is one of the largest coffee-producing regions in Indonesia, particularly in Central Aceh Regency, renowned for producing high-quality Gayo

coffee. The coffee production process in the Gayo Highlands involves the cultivation, and harvesting of coffee cherries, and processing them into coffee powder or grounds [10]. Inevitably, these processes generate a significant number of solid by-products with low economic value. The primary waste materials derived from coffee production include coffee husks, pulp, and spent coffee grounds [11].

Coffee processing generates substantial amounts of waste annually, including coffee pulp, husks, and spent coffee grounds, which are often discarded without proper treatment. According to Gouvea *et al.*, the global coffee industry produces approximately 6 million tons of spent coffee grounds annually, which poses environmental challenges due to its high organic content and potential to release harmful greenhouse gases if not managed properly [12]. This waste, however, holds significant potential for valorization due to its rich carbon content, making it an excellent precursor for activated carbon production. Activated carbon derived from coffee waste presents a compelling option due to its high surface area, porosity, and potential for chemical modifications, which enhance the material's ability to interact with MgH_2 . This aligns with research by Campos-Vega *et al.*, and others, which emphasize the valorization of coffee waste for energy storage applications, reducing environmental impact while creating high-performance materials [13].

In our study, coffee industry waste was selected as the raw material for activated carbon production due to its abundance, low cost, and high carbon content. This aligns with Sustainable Development Goals (SDGs) by promoting waste-to-value processes and reducing the environmental footprint of the coffee industry [14].

Among the diverse range of available catalytic materials, carbon-based catalysts have gained significant attention. Their lightweight nature, excellent chemical stability and high surface area make them highly suitable for this application. In particular, activated carbon (AC) has proven to be especially effective in enhancing the hydrogen storage properties of MgH_2 . AC promotes both the decomposition and reformation of MgH_2 , enabling these processes to take place at lower temperatures, thus optimizing the overall performance of hydrogen storage [15], [16].

In recent years, utilizing agricultural waste as a resource for producing activated carbon (AC) has emerged as a promising and sustainable strategy. This

innovative approach leverages materials such as coconut shells, palm oil residues, and coffee waste, which can be effectively transformed into activated carbon through chemical activation. This process not only promotes environmental sustainability by recycling agricultural by-products but also produces high-performance catalysts for hydrogen storage [17]–[24]. Among these materials, coffee waste, including both pulp and parchment, stands out as an exceptional feedstock for activated carbon production. By repurposing by-products of the coffee agro-industry, this approach enhances waste management practices while actively supporting the development of a circular economy. In doing so, it reduces environmental impact and unlocks new opportunities for innovation and economic growth in agricultural sectors.

Various agro-industrial wastes, such as coconut shells, nutshells, palm oil residue, olive oil residue, and coffee plant residues, have been utilized as raw materials for producing AC [25]–[28]. Jin *et al.*, reported producing AC from chemically activated coconut shells, achieving samples with varying degrees of porosity and a maximum hydrogen adsorption capacity of 0.85 wt% at 100 bar and 298 K [29]. Schaefer *et al.*, synthesized AC from olive stones using KOH as the activating agent, achieving hydrogen uptake ranging from 0.19 to 0.42 wt% at room temperature 298 K [21]. Similarly, Nurmalita *et al.*, developed AC from Robusta coffee pulp through chemical activation with NaOH and ZnCl₂, concluding that it is suitable for hydrogen storage applications [19].

Activated carbon derived from coffee waste presents a compelling option due to its high surface area, porosity, and potential for further chemical modifications. These characteristics enhance the material's ability to interact with MgH₂, thereby improving hydrogen adsorption and desorption kinetics. Furthermore, the chemical activation process, typically involving alkaline agents such as potassium hydroxide (KOH) or sodium hydroxide (NaOH), can be tailored to optimize the surface properties of the activated carbon, making it a more effective catalyst.

This study examines the potential of activated carbon derived from Arabica coffee pulp and parchment as a catalyst to enhance the hydrogen storage properties of MgH₂. Coffee waste-derived activated carbons were chemically activated using KOH and NaOH solutions, and their catalytic

effectiveness was evaluated through the preparation of MgH₂ composites. A range of characterization techniques, including differential scanning calorimetry (DSC), thermogravimetric analysis (TGA), scanning electron microscopy (SEM), and X-ray diffraction (XRD), was employed. The findings provide valuable insights into the role of coffee waste-derived activated carbon in lowering the dehydrogenation temperature and improving the kinetics of MgH₂, thus offering more efficient and sustainable hydrogen storage solutions.

Moreover, this research aligns with the increasing focus on utilizing biomass waste as a resource for advanced materials in energy storage applications. Waste-to-value strategies, such as converting coffee agro-industry residues into activated carbon, deliver substantial environmental benefits while providing economic advantages by supplying low-cost, sustainable catalysts for hydrogen storage technologies. The results of this study could drive future advancements in renewable energy storage, particularly in solid-state hydrogen storage technologies and other hydrogen-based energy systems.

2 Material and Methods

2.1 Materials

The coffee pulp and parchment as the raw materials were obtained from solid waste of Arabica Gayo coffee production located in Aceh Tengah Regency, Indonesia. Magnesium Hydride (MgH₂) powder, with 99.9% purity and a particle size of 50 μm (Sigma Aldrich), was used as a solid-state hydrogen storage material. Other chemicals included a 0.1 N iodine solution (Sigma Aldrich). The activator solutions were 2% to 4% of KOH (Merck) and NaOH (Merck), respectively. Distilled water was used to remove residues and acids during the preparation of activated carbon.

2.2 Composite preparation

In this study, we utilized pure MgH₂ powder with 99.9% purity and a particle size of 50 μm (Sigma Aldrich) along with activated carbon (AC) derived from coffee pulp and parchment. The coffee pulp and parchment were sourced from a local coffee agro-industry in Takengon, Aceh, and processed into AC through a two-step procedure: pyrolysis and chemical activation.

In the first step, the coffee pulp and parchment were washed thoroughly and soaked in water for 20 h. After soaking, the materials were sun-dried to remove residual moisture. The dried materials were then subjected to slow pyrolysis at 400 °C for 80 min, producing biochar. The biochar was chemically activated using KOH and NaOH solutions, with concentrations ranging from 2% to 4%.

In the second step, MgH₂ was catalyzed with 5 wt% AC using an intensive mechanical alloying method. The composites were prepared with a high-energy planetary ball mill (Fritsch, P6), employing a ball-to-powder ratio (BPR) of 10:1. The milling process was carried out for three hours at a rotational speed of 350 rpm. Table 1 provides a summary of the sample codes and relevant details for each sample.

Table 1: List sample code and information.

No	Sample Code	Materials
1.	CPAC-N2	Coffee pulp AC catalyst with NaOH 2% solution chemical activation
2.	CPAC-N3	Coffee pulp AC catalyst with NaOH 3% solution chemical activation
3.	CPAC-N4	Coffee pulp AC catalyst with NaOH 4% solution chemical activation
4.	CPAC-K2	Coffee pulp AC catalyst with KOH 2% solution chemical activation
5.	CPAC-K3	Coffee pulp AC catalyst with KOH 3% solution chemical activation
6.	CPAC-K4	Coffee pulp AC catalyst with KOH 4% solution chemical activation
7.	CHAC-N2	Coffee parchment AC catalyst with NaOH 2% solution chemical activation
8.	CHAC-N3	Coffee parchment AC catalyst with NaOH 3% solution chemical activation
9.	CHAC-N4	Coffee parchment AC catalyst with NaOH 4% solution chemical activation
10.	CHAC-K2	Coffee parchment AC catalyst with KOH 2% solution chemical activation
11.	CHAC-K3	Coffee parchment AC catalyst with KOH 3% solution chemical activation
12.	CHAC-K4	Coffee parchment AC catalyst with KOH 4% solution chemical activation
13.	MgH ₂ + 5 wt % CPAC-N2	MgH ₂ catalyzed with 5 wt% CPAC-N2
14.	MgH ₂ + 5 wt % CPAC-K2	MgH ₂ catalyzed with 5 wt% CPAC-K2
15.	MgH ₂ + 5 wt % CHAC-N3	MgH ₂ catalyzed with 5 wt% CHAC-N3
16.	MgH ₂ + 5 wt % CHAC-K2	MgH ₂ catalyzed with 5 wt% CHAC-K2

2.3 Testing and characterization methods

Fourier Transform Infrared Spectroscopy (FTIR) was conducted utilizing a Shimadzu FTIR-8400S spectrophotometer to analyze the functional groups present in the materials. For this analysis, samples were prepared by combining the material with potassium bromide (KBr) in a 1:200 weight ratio, and the resulting mixture was compressed into pellets. The spectra were recorded within the wavenumber range of 350–4000 cm⁻¹, achieving a resolution of 4 cm⁻¹ over 32 scans.

The iodine number, which serves as an indicator of the porosity of activated carbon (AC), was determined by measuring the quantity of iodine adsorbed per gram of carbon. This assessment adhered to the SNI 06-3730-1995 standard method.

Thermogravimetric analysis (TGA) was performed using the Shimadzu DTG-60 system to evaluate the thermal stability and composition of the materials. Each sample, weighing approximately 5–10 mg, was placed in a heat-resistant crucible and subjected to heating in a nitrogen atmosphere (20

mL/min) up to 1000 °C, at a consistent heating rate of 10 °C/min.

X-ray diffraction (XRD) analysis was carried out with a Shimadzu Maxima-X 7000 diffractometer, employing a Cu K α X-ray source at 40 kV and 30 mA. Data were collected over the 2 θ range of 5°–80°, and phase identification along with data processing was performed using DIFFRAC.EVA software. This analysis provided valuable insights into the crystalline phases and mineral composition of the samples.

Additionally, scanning electron microscopy (SEM) and energy-dispersive X-ray spectroscopy (EDS) were employed to investigate the surface morphology and elemental composition of the samples. SEM analysis was conducted using a JEOL 6510LV microscope, operating at accelerating voltages ranging from 0.5 to 30 kV. The samples were mounted on carbon disks and examined under both low vacuum (LV) and high vacuum (HV) conditions. EDS analysis was utilized to ascertain the elemental composition, while SEM imaging supplied detailed information regarding the pore structures and morphology of the activated carbon.

3 Results and Discussion

3.1 AC catalyst properties

3.1.1 FTIR Analysis

Figure 1 illustrates the Fourier Transform Infrared (FTIR) spectra of activated carbon (AC) derived from coffee pulp and coffee parchment through a chemical activation using KOH and NaOH solutions. The primary objective of obtaining the FTIR spectra is to identify and analyze the surface functional groups present in the activated carbon material. FTIR analysis was performed on four selected samples (CPAC-N2, CPAC-K2, CHAC-N3, and CHAC-K2) that exhibited excellent iodine adsorption capacities, suggesting an increased micropore content and reactivity. Such properties are vital for improving MgH_2 hydrogen storage capabilities. This targeted approach provided in-depth insights into the chemical functionalities of the most promising samples while effectively utilizing the study's resources. The FTIR spectra have several distinct features. A notable band at 3639 cm^{-1} is attributed to the presence of free hydroxyl (-OH) groups, which are essential for potential interactions with adsorbate molecules. This band is commonly observed in biomass-derived carbon material as reported in the literature [30], [31]. In addition, weak intensity peaks in the $2900\text{--}2800\text{ cm}^{-1}$ range correspond to the aldehyde functional group, indicating the presence of organic compounds that contribute to adsorption processes. A significant band at 2400 cm^{-1} represents the carboxylic acid functional group, which enhances the reactivity of the activated carbon surface. The spectral region between $1700\text{--}1600\text{ cm}^{-1}$ showcases the carbonyl (C=O) stretching vibration, characteristic of various functional groups such as aldehydes, esters, ketones, and carboxylic groups. Vibrations associated with caffeine are also in this region [32].

The aromatic C=C stretching vibrations are evident between $1600\text{--}1475\text{ cm}^{-1}$, indicating aromatic structures within the activated carbon matrix. A

distinct C-O stretching peak near 1000 cm^{-1} suggests the presence of ether or alcohol functionalities. Additionally, a sharp peak in the $800\text{--}600\text{ cm}^{-1}$ range signifies chloride compounds, which may derive from the precursors or activation chemicals used during processing.

Additional features include peaks around 3055 cm^{-1} , linked to the symmetric and asymmetric C-H bending vibrations associated with $-\text{CH}_2$ and $-\text{CH}_3$ groups, confirming the organic nature of the activated carbon. The adsorption peak near 1591 cm^{-1} corresponds to C=C stretching vibrations found in aromatic rings, which are characteristic of carbonaceous materials. Strong bands at 1423 cm^{-1} are attributed to C-H bending vibrations in alkyl groups such as $-\text{CH}_3$, suggesting a notable contribution of lignin from the original coffee pulp and parchment materials. Peaks in the $876\text{--}761\text{ cm}^{-1}$ range indicate out-of-plane C-H bending vibration in aromatic rings, further underscoring the aromatic nature of the activated carbon.

Overall, the FTIR spectra highlight a range of oxygen-containing functional groups, including hydroxyl, carboxyl, and carbonyl groups. These groups significantly enhance the adsorption capacity of activated carbon by increasing its surface reactivity and enabling effective interaction with target molecules or pollutants [29]. A comparison of the FTIR spectra of activated carbon derived from coffee parchment and coffee pulp reveals sharper peaks at 1591 cm^{-1} in the parchment sample, indicating a higher abundance or quality of aromatic structures. Additionally, a slight variation in the intensity of the carbonyl C=O stretching vibration ($1700\text{--}1600\text{ cm}^{-1}$) suggests a more pronounced presence of caffeine in the coffee parchment sample.

These findings demonstrate that the chemical activation process using KOH and NaOH preserves the surface functional groups of the activated carbon, maintaining the unique chemical characteristics of both coffee pulp and parchment precursors after activation.

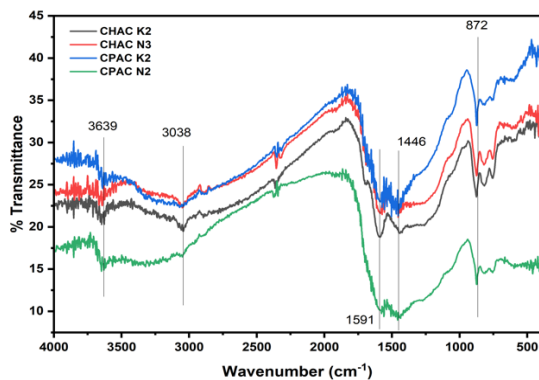


Figure 1: FTIR Spectra of coffee pulp and parchment AC.

3.1.2 The iodine adsorption capacity

The iodine number test measures the micropore content of activated carbon, indicating its adsorption capacity. For hydrogen storage, micropores are essential as they provide high surface area and enable effective hydrogen adsorption. However, mesopores also play a significant role in facilitating the diffusion of hydrogen molecules, thereby enhancing the overall storage performance. While the current study focuses on iodine adsorption as a proxy for micropore analysis, a more detailed evaluation using Brunauer–Emmett–Teller (BET) analysis is recommended to assess the complete pore size distribution and validate the suitability of these activated carbons for hydrogen storage applications.

The chemical activation method using KOH and NaOH has practical implications for the iodine adsorption capacity of AC. This research shows that the use of KOH as an activator yields superior iodine adsorption performance compared to NaOH (Figure 2). However, our findings indicate that increasing the concentration of KOH and NaOH beyond certain thresholds does not significantly improve iodine adsorption.

For instance, when a 4% NaOH solution was used to activate coffee parchment AC, the iodine adsorption capacity decreased, suggesting that NaOH concentrations exceeding 3% are not optimal for activating coffee pulp and parchment. On the other hand, higher concentrations of KOH did not significantly impact iodine adsorption, although the effect was more pronounced in coffee pulp AC, where adsorption decreased at elevated KOH concentrations.

The differences between KOH and NaOH can be attributed to their distinct etching behaviors during activation. KOH penetrates the carbon matrix more effectively due to its smaller ionic radius, leading to a more uniform micropore structure and higher surface area. In contrast, NaOH, with its larger ionic radius, may block pores or cause over-etching at higher concentrations, resulting in micropore collapse and reduced adsorption capacity. Furthermore, samples treated with KOH exhibit better thermal stability, which helps maintain the optimized pore structure and adsorption properties. These observations underline the effectiveness of KOH as a superior activating agent for producing high-performance activated carbons.

The observed decrease in iodine adsorption capacity at higher NaOH concentrations (>3%) can be attributed to over-etching, where excessive NaOH erodes the carbon structure, collapsing micropores and reducing adsorption sites. Additionally, the larger ionic radius of Na⁺ compared to K⁺ may contribute to pore blockage, limiting effective activation at higher concentrations [33]. Conversely, KOH demonstrates a more controlled etching effect due to its smaller ionic radius and better penetration into the carbon matrix. This enables the formation and preservation of optimal pore structures even at higher concentrations, as reflected in the consistent performance of KOH-activated samples. These findings suggest that KOH is a more robust activating agent for achieving high-performance activated carbons [34], [35].

The highest iodine adsorption was achieved with coffee parchment AC activated using 2% KOH (CHAC-K2) reaching 888.3 mg/g, followed by coffee parchment AC activated with 3% NaOH (CHAC-N3) at 837.54 mg/g. For coffee pulp AC, the best iodine adsorption was observed with 2% KOH (CPAC-K2) at 799.47 mg/g and 2% NaOH (CPAC-N2) at 532.98 mg/g.

These findings highlight the importance of optimizing activator type and concentration to maximize adsorption performance. The results are particularly relevant for professionals in environmental science and materials engineering, offering insight into producing high-performance activated carbon. Additionally, this study aligns with existing literature, which identifies KOH as a highly effective activation agent for producing activated carbon with commercial-grade adsorptive capacities [36], [37].

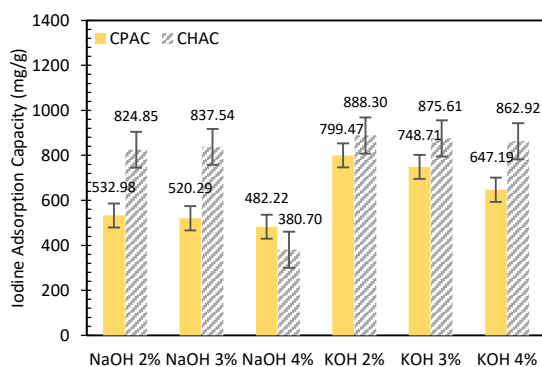


Figure 2: Iodine adsorption capacity of coffee pulp and parchment AC.

3.1.3 SEM-EDS analysis

Figure 3 presents SEM images of AC samples derived from coffee pulp and parchment, which were chemically activated using NaOH and KOH solutions. Coffee pulp AC exhibits a flat, rough surface with poorly developed pores, which are mostly round and layered in multiple layers. In contrast, coffee parchment AC displays better pore formation, though the surface remains rough and irregular.

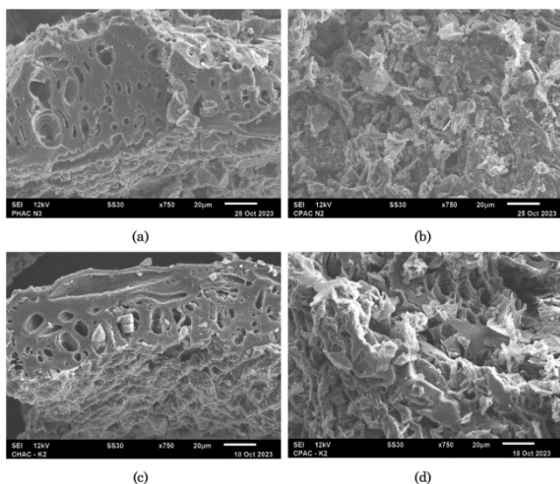


Figure 3: SEM analysis of (a) CHAC-N3, (b) CPAC-N2, (c) CHAC-K2 and (d) CPAC-K2.

SEM analysis suggests that coffee parchment AC exhibits more and better-defined pores compared to coffee pulp AC. However, as SEM provides only qualitative insights into surface morphology, quantitative analysis such as Brunauer–Emmett–Teller (BET) method is required to confirm pore

volumes and distribution, including micropores and mesopores. The size and shape of the activated carbon surface play a crucial role in determining its adsorption capacity. Micropores significantly contribute by providing a high surface area, while mesopores facilitate diffusion pathways for hydrogen molecules. The activated carbon derived from coffee parchment, which displays a more interconnected and developed pore structure as seen in SEM images, showcases a higher adsorption capacity. This is further validated by its outstanding iodine adsorption results. Moreover, the rough and irregular surface morphology of this AC provides additional active sites for hydrogen interaction. These structural characteristics underscore the necessity of optimizing pore size distribution and surface features to enhance the adsorption capacity in hydrogen storage applications.

This recommendation aligns with the study’s aim of enhancing hydrogen storage properties and will serve as a focus for future work. These findings, nonetheless, are consistent with previous research, such as Campos *et al.*, who reported that AC produced from coffee parchment activated with CaCO₃ exhibited a rough, randomly porous surface [37]. Furthermore, the type of chemical activator significantly influences pore formation. AC activated with KOH produces a greater number of larger pores compared to AC activated with NaOH [38]. Chia *et al.*, studied AC derived from rice husk and found that KOH activation resulted in enhanced surface porosity and increased pore volume compared to NaOH activation [39]. This finding demonstrates the effectiveness of KOH as an activation agent for producing AC, and that coffee parchment undergoes better thermal decomposition than coffee pulp.

3.1.4 Thermogravimetric analysis of AC

TGA-DTG analysis was conducted to assess the thermal stability of the synthesized activated carbon (AC) sample, as shown in Figure 4. The initial weight loss, observed between 30 and 150 °C, ranged from 5% to 15% of the sample’s weight. This relatively higher percentage of weight loss indicates the enhanced adsorptive properties of the AC, likely due to its microporous structure, which allows it to adsorb more water molecules compared to the relatively non-porous charcoal.

The second stage of weight loss was observed between 150 and 900 °C, with a reduction of 10% to 25%. This was primarily due to the pyrolysis of organic

volatiles and the decomposition of lignin within the carbon matrix. Significant differences were observed in the thermal decomposition behavior between the two raw materials. Specifically, activated carbon produced from coffee pulp showed a higher degree of mass loss compared to that derived from coffee parchment. The TGA curve indicates that AC derived from coffee parchment exhibits significantly superior thermal stability compared to that from coffee pulp.

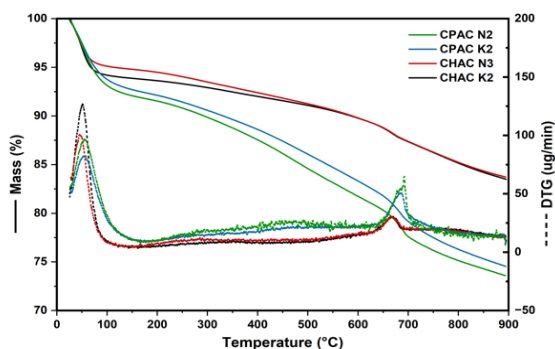


Figure 4: TGA and DTG curves of coffee pulp and parchment AC.

The use of KOH and NaOH as activators did not significantly impact the thermal stability of the activated carbon made from coffee parchment. However, NaOH showed a greater effect on the activated carbon derived from coffee pulp. Notably, KOH exhibited lower levels of thermal decomposition compared to NaOH.

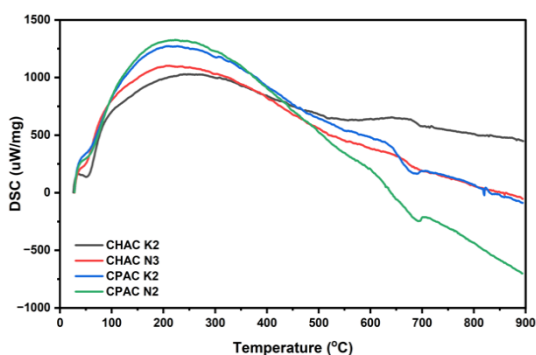


Figure 5: DSC curve of coffee pulp and parchment AC.

The Differential Scanning Calorimetry (DSC) curve (Figure 5) provides critical insights into the thermal properties of the synthesized activated carbon (AC) samples. The analysis highlights key endothermic and exothermic transitions, indicating the material's thermal stability and behavior under

heating conditions. Initially, an endothermic peak at a lower temperature range of 30–150 °C indicates water desorption from the material's surface, a common characteristic of activated carbons with microporous structures. This peak suggests the presence of adsorbed moisture or low molecular weight species within the carbon matrix [34].

Further along the temperature range, the DSC curve for activated carbon (AC) derived from coffee pulp shows a noticeable exothermic peak, typically occurring between 150 °C and 500 °C. This peak marks the initiation of decomposition or the release of volatiles from the material. The intensity of this peak is generally associated with the pyrolysis of organic volatiles and the degradation of lignin within the structure. In contrast, the AC derived from coffee parchment exhibits a much lower intensity for this peak, indicating better thermal stability. This difference can be attributed to the structural variations between the raw materials or the activation processes used [40], [41], as coffee parchment generally possesses a more stable structure than coffee pulp.

At temperatures ranging from 600 and 900 °C, an exothermic reaction indicates, further decomposition, likely from the breakdown of more stable components in the activated carbon, such as aromatic structures and leftover organic compounds. This could also reflect the thermal degradation of inorganic impurities introduced during the synthesis [42]. The activated carbon derived from coffee pulp undergoes more significant thermal decomposition in this range when compared to that derived from coffee parchment, which shows better thermal resistance. The thermal resistance of AC is heavily influenced by variations in pore structures and the chemical compositions of the material [43].

The DSC curve for materials activated by KOH and NaOH reveals significant trends. Although both activators improve the adsorption properties of activated carbon (AC), they affect thermal stability differently. For AC derived from coffee pulp, using NaOH leads to a more pronounced exothermic peak that indicates greater decomposition, while the KOH-activated AC shows a lower decomposition rate [43]. This suggests that the choice of activation agent significantly influences the thermal resistance of the carbon, with KOH treatment producing a more thermally stable material. This finding is consistent with research by Sitthikhankaew *et al.*, in which KOH-impregnated activated carbon adsorbs more H₂S as a result of its higher porosity [44].

3.2 MgH₂ composite properties

3.2.1 Thermogravimetric analysis of MgH₂ composites

Figure 6 presents the TGA curve of MgH₂ combined with 5 wt.% activated carbon (AC) sourced from both coffee pulp and parchment, analyzed at a heating rate of 10 °C/min under a nitrogen flow of 20 mL/min. The TGA analysis indicated a significant weight loss in the MgH₂ composite sample between 300 °C and 450 °C, signaling the onset of MgH₂ dehydrogenation. This weight loss was consistent across all samples. However, it was observed that the AC catalyst derived from coffee parchment began to decompose at a slightly lower temperature than that of the composite MgH₂ combined with the coffee pulp catalyst.

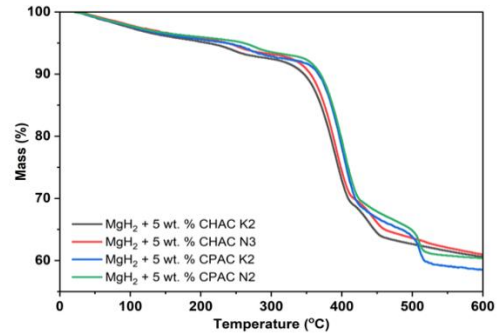
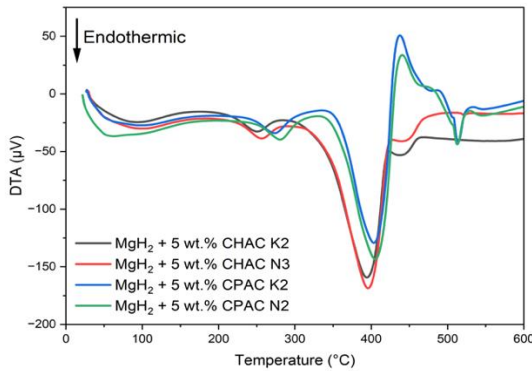
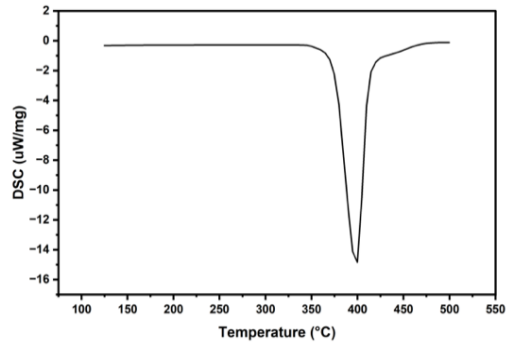


Figure 6: TGA curve of MgH₂ + 5wt.% coffee pulp and parchment AC with heating rate 10 °C/min under 20 mL/min of nitrogen flow.



(a)



(b)

Figure 7: (a) DTA curve of MgH₂ doped with AC catalysts from coffee pulp and parchment, with 'T onset,' 'T peak,' and 'T endset' values marked for comparison. (b) DTA curve of pure MgH₂ under identical conditions.

Figure 7(a) illustrates the DTA analysis of MgH₂ doped with AC catalysts from both coffee pulp and parchment, conducted under the same conditions (heating rate of 10 °C/min and nitrogen flow rate of 20 mL/min). The DTA results revealed a pronounced endothermic peak in the 300–450 °C range for all four materials, corresponding to the hydrogen release process occurring in each MgH₂ sample [45]. For

comparison, pure MgH₂ was also analyzed (Figure 7(b)). To enhance clarity and provide a direct comparison, the 'T onset,' 'T peak,' and 'T endset' values from Table 2 have been added as annotations in Figure 7. These values illustrate the differences in thermal behavior between MgH₂ composites and pure MgH₂, emphasizing the role of activated carbon in reducing the dehydrogenation temperature.

Table 2: Summary of dehydrogenation endset and onset temperature.

Materials	T onset (°C)	T peak (°C)	T endset (°C)	T onset (°C)	T endset (°C)
MgH ₂	373.90	398.36	414.49		
MgH ₂ + 5 wt.% CHAC-K2	342.36	400.32	418.44	346.44	418.09
MgH ₂ + 5 wt.% CHAC-N3	346.16	401.26	420.33	347.48	420.01
MgH ₂ + 5 wt.% CPAC-K2	356.56	410.57	430.45	361.09	430.60
MgH ₂ + 5 wt.% CPAC-N2	354.21	411.77	432.43	359.24	432.93

The dehydrogenation process was distinctly observed, and it was found that the addition of AC from both coffee pulp and parchment lowered the onset temperature for MgH_2 dehydrogenation (Table 2). Notably, the AC catalyst from coffee parchment exhibited slower onset and peak temperatures compared to that from coffee pulp. For instance, the $\text{MgH}_2 + 5$ wt.% coffee pulp AC catalysts (CHAC-K2 and CHAC-N3) had onset temperatures of 342.36°C and 346.16°C , respectively, while the $\text{MgH}_2 + 5$ wt.% coffee parchment AC catalysts (CPAC-K2 and CPAC-N2) had slightly higher onset temperatures of 356.56°C and 354.21°C .

3.2.2 XRD analysis of MgH_2 composites

The XRD spectra of MgH_2 composites doped with activated carbon derived from coffee pulp and parchment show the absence of additional peaks corresponding to AC, likely due to its limited quantity or amorphous nature (Figure 8). This observation aligns with previous studies, where the incorporation of carbon-based additives was shown to reduce the dehydrogenation temperature and improve the kinetics of MgH_2 without significantly altering its crystal structure [46].

The effectiveness of coffee-waste-derived activated carbon in enhancing MgH_2 properties compares favorably with results from other studies. For example, Jin *et al.*, reported hydrogen adsorption capacities of 0.85 wt% for activated carbon derived from coconut shells [29], while Schaefer *et al.*, observed uptake ranging from 0.19 to 0.42 wt% in olive-stone-derived activated carbons under similar conditions [21]. In this study, coffee parchment AC, particularly CHAC-K2, significantly reduced the dehydrogenation onset temperature of MgH_2 to 342.36°C , demonstrating a marked improvement over pure MgH_2 . These findings underscore the potential of coffee-waste-derived AC as a competitive and sustainable alternative for hydrogen storage applications.

Furthermore, the chemical activation process used in this study, particularly with KOH, has been shown to create an optimal balance of micropores and mesopores, which are critical for hydrogen diffusion and adsorption. Such structural enhancements directly contribute to the observed improvements in hydrogen desorption properties, consistent with findings from other studies on carbon-based catalysts.

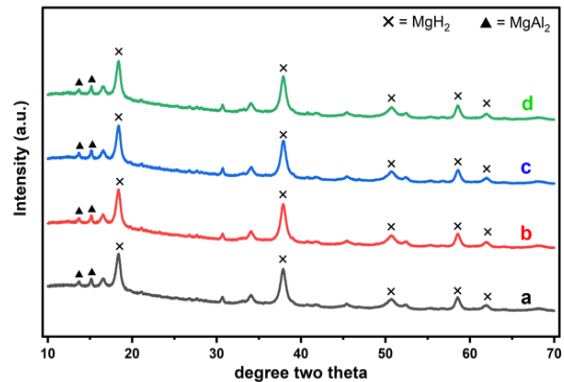


Figure 8: XRD patterns of (a) $\text{MgH}_2 + 5$ wt.% CHAC-K2, (b) $\text{MgH}_2 + 5$ wt.% CHAC-N3, (c) $\text{MgH}_2 + 5$ wt.% CPAC-K2 and (d) $\text{MgH}_2 + 5$ wt.% CPAC-N2.

3.2.3 SEM-EDS analysis of MgH_2 composites

Figure 9 presents Scanning Electron Microscopy (SEM) images of MgH_2 mixed with 5 wt.% AC. The SEM images (Figure 9) include highlighted regions corresponding to the areas analyzed for EDS spectra, as shown in Figure 10. This ensures a clear correlation between the morphological and compositional data. The SEM micrographs show a distinct contrast, with several small particles, likely AC nanoparticles, scattered across and around larger MgH_2 particles. This observation indicates that ball milling effectively reduces particle size, creating new active surfaces within the nano-composite. The existence of these smaller particles and the increased surface area are crucial for enhancing the efficiency of the dehydrogenation and hydrogen adsorption processes.

The SEM images also suggest that the reduction in particle size arises from an inhomogeneous distribution, which is expected to improve the kinetics of MgH_2 since smaller particles facilitate faster hydrogen diffusion. This size reduction is believed to promote active nucleation, likely triggered by the mechanical milling of pure MgH_2 with AC. The milling process reduces the diffusion distance for hydrogen atoms and creates clean, highly reactive surfaces, essential for effective hydrogen release and adsorption [47], [48]. Additionally, all prepared samples were analyzed for their elemental composition using Energy-Dispersive X-ray (EDX) spectroscopy, which was conducted alongside the SEM analysis.

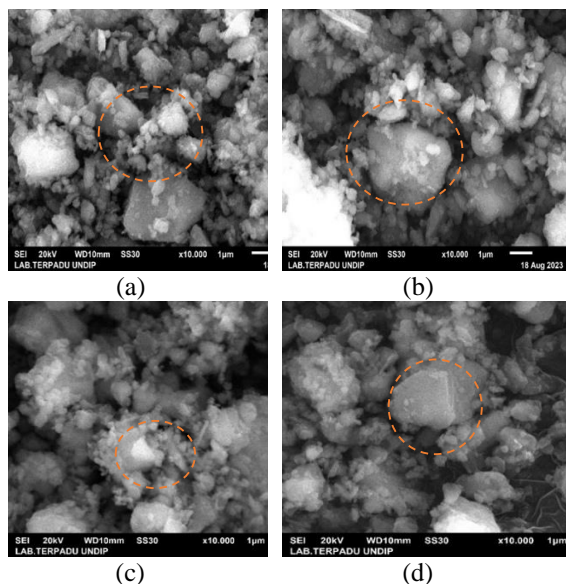


Figure 9: SEM of (a) $\text{MgH}_2 + 5 \text{ wt.}\% \text{ CHAC-K2}$, (b) $\text{MgH}_2 + 5 \text{ wt.}\% \text{ CHAC-N3}$, (c) $\text{MgH}_2 + 5 \text{ wt.}\% \text{ CPAC-K2}$ and (d) $\text{MgH}_2 + 5 \text{ wt.}\% \text{ CPAC-N2}$.

Figure 10 illustrates the elemental composition of the $\text{MgH}_2 + \text{AC}$ nanocomposites as determined by EDS analysis. The results confirm the successful integration of activated carbon into the MgH_2 matrix, as evidenced by the high carbon (C) content, alongside magnesium (Mg) and oxygen (O_2). Minor elements, such as aluminium (Al), calcium (Ca), iron (Fe), and copper (Cu), were also detected, likely originating from the precursor materials or the ball-milling process.

The incorporation of 5 wt.% activated carbon (AC) into MgH_2 represents an optimized composition for improving hydrogen storage performance, as supported by the findings of this study. While the preparation process, including pyrolysis, chemical activation, and ball milling, involves multiple steps, its scalability depends on several factors. Firstly, cost of raw materials, coffee pulp and parchment are abundant agro-industrial wastes, offering a low-cost feedstock for producing AC, which supports economic feasibility. Secondly, energy requirements, low-temperature pyrolysis and chemical activation processes were intentionally chosen for their relatively

lower energy demands compared to high-temperature treatments, improving overall cost efficiency. Thirdly, ball milling, although extensive ball milling is resource-intensive, advancements in high-energy milling technologies could significantly reduce processing time and energy consumption, enhancing scalability. To further improve the techno-economic feasibility, the integration of renewable energy sources for powering pyrolysis and milling processes could lower operation costs. Additionally, exploring alternative mechanical alloying techniques or chemical modifications may streamline production.

Thus, while the process presents some challenges for large-scale implementation, its reliance on low-cost raw materials and the potential for process optimization make it a promising candidate for industrial applications. Further studies focusing on scaling up these processes and conducting a comprehensive cost-benefit analysis will provide valuable insights into its viability.

The sample $\text{MgH}_2 + 5 \text{ wt.}\% \text{ CPAC-K2}$ contains 66.71% carbon and 19.26% magnesium. For the $\text{MgH}_2 + 5 \text{ wt.}\% \text{ CPAC-N}_2$ sample, the carbon content is 54.56% and magnesium is 26.93%. In the $\text{MgH}_2 + 5 \text{ wt.}\% \text{ CHAC-K2}$ sample, the carbon content is 58.65% and magnesium is 23.69%. Meanwhile, the $\text{MgH}_2 + 5 \text{ wt.}\% \text{ CHAC-N}_3$ sample has 59.90% carbon and 23.20% magnesium.

The high carbon content across all samples highlights the stability of the activated biochar during the integration process with MgH_2 , which is crucial for enhancing the material's hydrogen storage performance.

This finding aligns with Zhang *et al.*, research, which states that carbon-rich biochar can enhance the hydrogenation and desorption kinetics of MgH_2 through interfacial interactions and the provision of ion diffusion pathways, thereby accelerating hydrogen release [35]. Additionally, the addition of activated biochar to MgH_2 improve the material's thermal stability by acting as a gas diffusion barrier and reducing degradation due to oxidation [49]. It shows the percentage of each element and confirms the successful incorporation of AC into the MgH_2 matrix, as well as its role in enhancing the material properties.

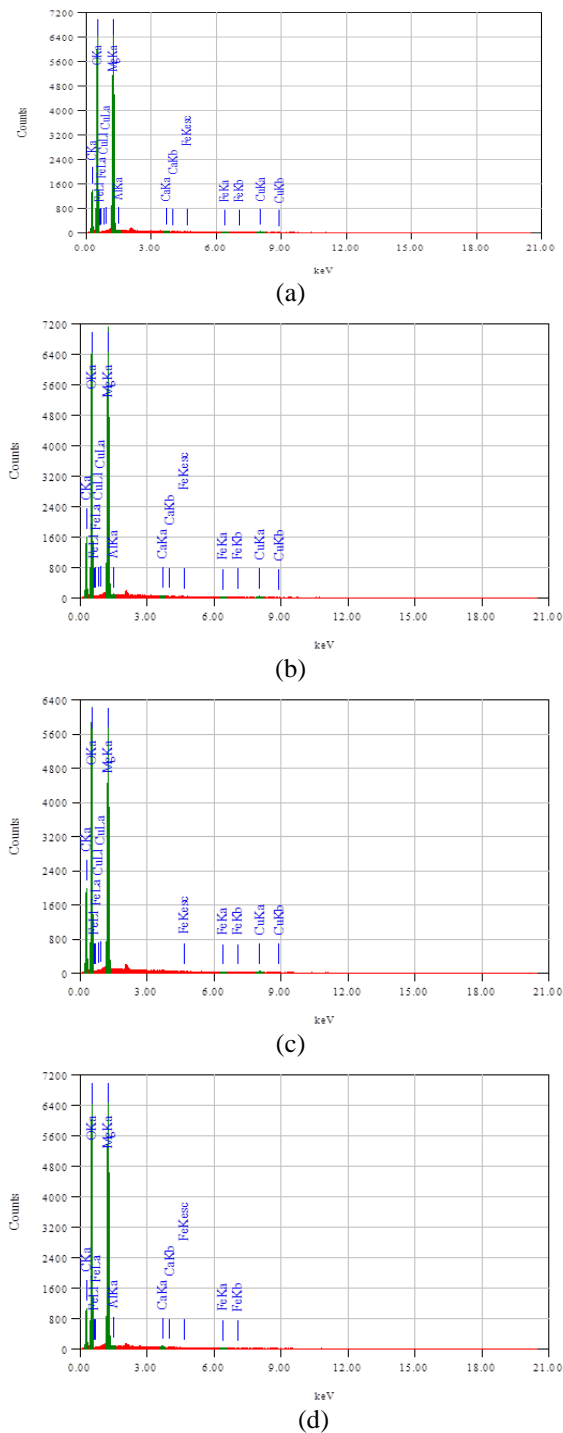


Figure 10: EDS of (a) MgH_2 + 5 wt.% CHAC-K2, (b) MgH_2 + 5 wt.% CHAC-N3, (c) MgH_2 + 5 wt.% CPAC-K2 and (d) MgH_2 + 5 wt.% CPAC-N2.

4 Conclusions

The innovative utilization of AC derived from coffee agro-industrial residues as a catalyst for hydrogen storage applications represents a significant advancement in the field of energy storage technology. Recent experimental investigations have demonstrated that incorporating AC produced specifically from coffee pulp and parchment markedly enhances the kinetic performance and overall characteristics of hydrogen desorption in magnesium hydride (MgH_2).

Through detailed thermal analysis of the MgH_2 -AC composite, it has been determined that the most favorable hydrogen storage properties can be obtained by mechanically milling MgH_2 with a concentration of 5 wt% activated carbon. This formulation resulted in a substantial reduction of the onset dehydrogenation temperature, which was observed to fall within the 342.36 to 356.56 °C range. Such a decrease is highly advantageous for practical applications, allowing for more efficient hydrogen release at lower temperatures. Moreover, the study further revealed that the introduction of 5 wt% of coffee parchment AC, which had been chemically activated using a 2% KOH solution, led to an even more pronounced reduction in the dehydrogenation temperature, lowering it to an impressive 342.36 °C.

This finding underscores the potential of utilizing coffee industry waste not only as a value-added product but also as a crucial component in developing advanced hydrogen storage solutions. As a result, this research opens up exciting pathways for enhancing hydrogen storage technologies, ultimately contributing to the advancement of renewable energy systems and promoting sustainability within the agro-industry.

Acknowledgments

The authors acknowledge the Directorate of Research, Technology, and Community Service, Ministry of Education, Culture, Research and Technology, Republic of Indonesia for their sponsorship under contract no. 028/E5/PG.02.00.PL/2023, sub-contract number 5/UN45.2.1/PT.01.03/V/2023. ZJ special thanks to S ejour Scientifique de Haut Niveau (SSHN) & Science et Impact Program 2024.

Author Contributions

A.S.: conceptualization, research design, funding acquisition, investigation, reviewing and editing; S.N.: investigation, methodology, writing an original draft; S.R.: project administration, data curation and data analysis; M.M. & Z.J.: conceptualization, writing—reviewing and editing. All authors have read and agreed to the published version of the manuscript.

Conflicts of Interest

The authors declare no conflict of interest.

References

- [1] K. Chawla, D. K. Yadav, P. Sharda, N. Lal, S. Sharma, and C. Lal, “Hydrogenation properties of MgH₂- x wt% AC (x=0, 5, 10, 15) nanocomposites,” *International Journal of Hydrogen Energy*, vol. 45, no. 44, pp. 23971–23976, 2020, doi: 10.1016/j.ijhydene.2019.09.022.
- [2] K. L. Lim, H. Kazemian, Z. Yaakob, and W. R. W. Daud, “Solid-state materials and methods for hydrogen storage: A critical review,” *Chemical Engineering and Technology*, vol. 33, no. 2, pp. 213–226, 2010, doi: 10.1002/ceat.200900376.
- [3] J. A. Bolarin, R. Zou, Z. Li, A. Munitywali, Z. Zhang, and H. Cao, “Recent path to ultrafine Mg/MgH₂ synthesis for sustainable hydrogen storage,” *International Journal of Hydrogen Energy*, vol. 52, pp. 251–274, 2023, doi: 10.1016/j.ijhydene.2023.04.234.
- [4] L. E. Klebanoff, K. C. Ott, L. J. Simpson, K. O’Malley, and N. T. Stetson, “Accelerating the understanding and development of hydrogen storage materials: A review of the five-year efforts of the three DOE hydrogen storage materials centers of excellence,” *Metallurgical and Materials Transactions E*, vol. 1, no. 2, pp. 81–117, 2014, doi: 10.1007/s40553-014-0011-z.
- [5] M. R. Usman, “Hydrogen storage methods: Review and current status,” *Renewable and Sustainable Energy Reviews*, vol. 167, Oct. 2022, Art. no. 112743, doi: 10.1016/j.rser.2022.112743.
- [6] M. Yang, R. Hunger, S. Berrettoni, B. Sprecher, and B. Wang, “A review of hydrogen storage and transport technologies,” *Clean Energy*, vol. 7, no. 1, pp. 190–216, Feb. 2023, doi: 10.1093/ce/zkad021.
- [7] L. Mulky, S. Srivastava, T. Lakshmi, E. R. Sandadi, S. Gour, N. A. Thomas, S. S. Priya, and K. Sudhakar, “An overview of hydrogen storage technologies – Key challenges and opportunities,” *Materials Chemistry and Physics*, vol. 325, Oct. 2024, Art. no. 129710, doi: 10.1016/j.matchemphys.2024.129710.
- [8] N. A. Ali and M. Ismail, “Advanced hydrogen storage of the Mg–Na–Al system: A review,” *Journal of Magnesium and Alloys*, vol. 9, no. 4, pp. 1111–1122, 2021, doi: 10.1016/j.jma.2021.03.031.
- [9] Malahayati, Nurmalita, Ismail, M. N. Machmud, and Z. Jalil, “Sorption behavior of MgH₂-Ti for Hydrogen storage material prepared by high pressure milling,” *Journal of Physics: Conference Series*, vol. 1882, no. 1, May 2021, Art. no. 012005, doi: 10.1088/1742-6596/1882/1/012005.
- [10] A. Setiawan, B. B. Sitepu, M., K. Anshar, S. Riskina, S. Nurjannah, and L. Hakim, “Converting arabica coffee parchment into value-added products: Technical and economic assessment,” *Coffee Science*, 2024, Art. no. e192185, doi: 10.25186/v19i2.2185.
- [11] A. H. Sarosa, V. Nurhadianty, N. H. F. Naufal Dian, F. N. Anita, A. F. Noerdinna, and S. D. Ainur Rizqy, “The kinetic study of dampit robusta coffee caffeine degradation by *Saccharomyces cerevisiae*,” *Applied Science and Engineering Progress*, vol. 17, no. 1, Jul. 2023, Art. no. 6891, doi: 10.14416/j.asep.2023.07.004.
- [12] B. M. Gouvea, C. Torres, A. S. Franca, L. S. Oliveira, and E. S. Oliveira, “Feasibility of ethanol production from coffee husks,” *Biotechnology Letters*, vol. 31, no. 9, pp. 1315–1319, Sep. 2009, doi: 10.1007/s10529-009-0023-4.
- [13] R. Campos-Vega, G. Loarca-Piña, H. A. Vergara-Castañeda, and B. D. Oomah, “Spent coffee grounds: A review on current research and future prospects,” *Trends in Food Science & Technology*, vol. 45, no. 1, pp. 24–36, Sep. 2015, doi: 10.1016/j.tifs.2015.04.012.
- [14] R. Raihan, A. Setiawan, L. Hakim, Muhammad, M. Arif, and H. Hosseiniamoli, “Preparation and characterization of active charcoal made from robusta coffee skin (*Coffea Canephora*),” *Journal of Chemical Engineering and Environment*, vol. 15, no. 2, pp. 104–110, 2020, doi: 10.23955/rkl.v15i2.17618.
- [15] M. Konarova, A. Tanksale, J. Norberto

- Beltramini, and G. Qing Lu, "Effects of nano-confinement on the hydrogen desorption properties of MgH_2 ," *Nano Energy*, vol. 2, no. 1, pp. 98–104, 2013, doi: 10.1016/j.nanoen.2012.07.024.
- [16] Q. Zhang, Y. Huang, M. Tiancai, K. Li, X. Wang, L. Jiao, H. Yuan, and Y. Wang, "Facile synthesis of small MgH_2 nanoparticles confined in different carbon materials for hydrogen storage," *Journal of Alloys and Compounds*, vol. 825, pp. 1–9, 2020, doi: 10.1016/j.jallcom.2020.153953.
- [17] H. Jin, Y. S. Lee, and I. Hong, "Hydrogen adsorption characteristics of activated carbon," *Catalysis Today*, vol. 120, no. 3–4, pp. 399–406, 2007, doi: 10.1016/j.cattod.2006.09.012.
- [18] W. Su, L. Zhou, and Y. Zhou, "Preparation of microporous activated carbon from raw coconut shell by two-step procedure," *Chinese Journal of Chemical Engineering*, vol. 14, no. 2, pp. 266–269, Apr. 2006, doi: 10.1016/S1004-9541(06)60069-4.
- [19] N. Nurmali, R. Raihan, Z. Jalil, S. Nur, and A. Setiawan, "The Physical and chemical properties of activated nanocarbon produced from Robusta (*Coffea Canephora*) coffee pulp under slow pyrolysis method," *Coffee Science*, vol. 17, pp. 1–10, 2023, doi: 10.25186/v17i.2019.
- [20] X. J. Lee, L. Y. Lee, S. Gan, S. Thangalazhy-Gopakumar, and H. K. Ng, "Biochar potential evaluation of palm oil wastes through slow pyrolysis: Thermochemical characterization and pyrolytic kinetic studies," *Bioresource Technology*, vol. 236, pp. 155–163, Jul. 2017, doi: 10.1016/j.biortech.2017.03.105.
- [21] S. Schaefer, A. Jeder, G. Sdanghi, P. Gadonneix, A. Abdedayem, M. Izquierdo, G. Maranzana, A. Ouederni, A. Celzard, and V. Fierro, "Oxygen-promoted hydrogen adsorption on activated and hybrid carbon materials," *International Journal of Hydrogen Energy*, vol. 45, no. 55, pp. 30767–30782, Nov. 2020, doi: 10.1016/j.ijhydene.2020.08.114.
- [22] K. L. Lim, H. Kazemian, Z. Yaakob, and W. R. W. Daud, "Solid-state materials and methods for hydrogen storage: A critical review," *Chemical Engineering & Technology*, vol. 33, no. 2, pp. 213–226, Feb. 2010, doi: 10.1002/ceat.200900376.
- [23] W. Riansa-ngawong, W. Savedboworn, and M. Suwansaard, "Optimization of hydrogen production from pickle bamboo shoot wastewater by *Rhodospseudomonas palustris* TN1," *KMUTNB International Journal of Applied Science and Technology*, vol. 8, no. 3, pp. 205–212, Jul. 2015, doi: 10.14416/j.ijast.2015.06.004.
- [24] N. A. Basha, T. Rathinavel, and H. Sridharan, "Activated carbon from coconut shell: Synthesis and its commercial applications - A recent review," *Applied Science and Engineering Progress*, vol. 16, no. 2, Jul. 2023, Art. no. 6152, doi: 10.14416/j.asep.2022.07.001.
- [25] M. Mohan, V. K. Sharma, E. A. Kumar, and V. Gayathri, "Hydrogen storage in carbon materials —A review," *Energy Storage*, vol. 1, no. 2, Apr. 2019, doi: 10.1002/est2.35.
- [26] L. S. Blankenship, N. Balahmar, and R. Mokaya, "Oxygen-rich microporous carbons with exceptional hydrogen storage capacity," *Nature Communications*, vol. 8, no. 1, p. 1545, Nov. 2017, doi: 10.1038/s41467-017-01633-x.
- [27] G. Sethia and A. Sayari, "Activated carbon with optimum pore size distribution for hydrogen storage," *Carbon*, vol. 99, pp. 289–294, Apr. 2016, doi: 10.1016/j.carbon.2015.12.032.
- [28] A. Fomkin, A. Pribylov, I. Men'shchikov, A. Shkolin, O. Aksyutin, A. Ishkov, K. Romanov, and E. Khozina, "Adsorption-based hydrogen storage in activated carbons and model carbon structures," *Reactions*, vol. 2, no. 3, pp. 209–226, Jul. 2021, doi: 10.3390/reactions2030014.
- [29] H. Jin, Y. S. Lee, and I. Hong, "Hydrogen adsorption characteristics of activated carbon," *Catalysis Today*, vol. 120, no. 3–4, pp. 399–406, Feb. 2007, doi: 10.1016/j.cattod.2006.09.012.
- [30] Z. Fona, Irvan, R. Tambun, Fatimah, and A. Setiawan, "Physico-chemical characteristics of coffee parchment and its combustion residue to delineate the components required for gasification catalyst," *Case Studies in Chemical and Environmental Engineering*, vol. 10, Dec. 2024, Art. no. 100991, doi: 10.1016/j.cscee.2024.100991.
- [31] H. Kristianto, A. A. Arie, R. F. Susanti, M. Halim, and J. K. Lee, "The effect of activated carbon support surface modification on characteristics of carbon nanospheres prepared by deposition precipitation of Fe-catalyst," *IOP Conference Series: Materials Science and Engineering*, vol. 162, no. 1, Nov. 2016, Art. no. 012034, doi: 10.1088/1757-899X/162/1/012034.
- [32] A. P. Craig, A. S. Franca, and L. S. Oliveira,

- “Discrimination between immature and mature green coffees by attenuated total reflectance and diffuse reflectance fourier transform infrared spectroscopy,” *Journal of Food Science*, vol. 76, no. 8, 2011, doi: 10.1111/j.1750-3841.2011.02359.x.
- [33] J. Alcañiz-Monge, M. del C. Román-Martínez, and M. Á. Lillo-Ródenas, “Chemical activation of lignocellulosic precursors and residues: what else to consider?,” *Molecules*, vol. 27, no. 5, p. 1630, Mar. 2022, doi: 10.3390/molecules27051630.
- [34] W. M. A. W. Daud, W. S. W. Ali, and M. Z. Sulaiman, “The effects of carbonization temperature on pore development in palm-shell-based activated carbon,” *Carbon*, vol. 38, no. 14, pp. 1925–1932, 2000, doi: 10.1016/S0008-6223(00)00028-2.
- [35] H. Zhang, Y. Yan, and L. Yang, “Preparation of activated carbon from sawdust by zinc chloride activation,” *Adsorption*, vol. 16, no. 3, pp. 161–166, Aug. 2010, doi: 10.1007/s10450-010-9214-5.
- [36] A. Khamkeaw, W. Sanprom, and M. Phisalaphong, “Activated carbon from bacterial cellulose by potassium hydroxide activation as an effective adsorbent for removal of ammonium ion from aqueous solution,” *Case Studies in Chemical and Environmental Engineering*, vol. 8, Dec. 2023, Art. no. 100499, doi: 10.1016/j.csee.2023.100499.
- [37] G. C. Figueroa, J. Perez, I. Block, S. Sagu, P. C. Saravia, A. Taubert, and H. Rawel, “Preparation of activated carbons from spent coffee grounds and coffee parchment and assessment of their adsorbent efficiency,” *Processes*, vol. 9, no. 8, p. 1396, Aug. 2021, doi: 10.3390/pr9081396.
- [38] Y. Gao, Q. Yue, B. Gao, and A. Li, “Insight into activated carbon from different kinds of chemical activating agents: A review,” *Science of The Total Environment*, vol. 746, Dec. 2020, Art. no. 141094, doi: 10.1016/j.scitotenv.2020.141094.
- [39] C. H. Chia, S. Zakaria, M. S. Sajab, and M. J. Saad, “Activated carbon produced from rice husk by NaOH and KOH activation and its adsorption in methylene blue,” *Advances in Agricultural and Food Research Journal*, pp. 1–13, 2022, doi: 10.36877/afrrj.a0000297.
- [40] M. Zięzio, B. Charnas, K. Jedynak, M. Hawryluk, and K. Kucio, “Preparation and characterization of activated carbons obtained from the waste materials impregnated with phosphoric acid(V),” *Applied Nanoscience*, vol. 10, no. 12, pp. 4703–4716, Dec. 2020, doi: 10.1007/s13204-020-01419-6.
- [41] J. Jjagwe, P. W. Olupot, E. Menya, and H. M. Kalibbala, “Synthesis and application of granular activated carbon from biomass waste materials for water treatment: A review,” *Journal of Bioresources and Bioproducts*, vol. 6, no. 4, pp. 292–322, Nov. 2021, doi: 10.1016/j.jobab.2021.03.003.
- [42] A. Świątkowski, E. Kuśmierk, K. Kuśmierk, and S. Błażewicz, “The influence of thermal treatment of activated carbon on its electrochemical, corrosion, and adsorption characteristics,” *Molecules*, vol. 29, no. 20, p. 4930, Oct. 2024, doi: 10.3390/molecules29204930.
- [43] G. Duran-Jimenez, J. Rodriguez, L. Stevens, S. Altarawneh, A. Batchelor, L. Jiang, and C. Dodds., “Single-step preparation of activated carbons from pine wood, olive stones and nutshells by KOH and microwaves: Influence of ultra-microporous for high CO₂ capture,” *Chemical Engineering Journal*, vol. 499, Nov. 2024, Art. no. 156135, doi: 10.1016/j.cej.2024.156135.
- [44] R. Sitthikhankaw, D. Chadwick, S. Assabumrungrat, and N. Laosiripojana, “Effect of KI and KOH Impregnations over Activated Carbon on H₂S Adsorption Performance at Low and High Temperatures,” *Separation Science and Technology*, vol. 49, no. 3, pp. 354–366, Feb. 2014, doi: 10.1080/01496395.2013.841240.
- [45] N. A. Ali, M. S. Yahya, N. Sazelee, M. F. M. Din, and M. Ismail, “Influence of nanosized CoTiO₃ synthesized via a solid-state method on the hydrogen storage behavior of MgH₂,” *Nanomaterials*, vol. 12, no. 17, 2022, doi: 10.3390/nano12173043.
- [46] N. C. Mazlan, M. A. A. H. Yap, M. Ismail, M. Yahya, N. Ali, N. Sazelee, and Y. Seok, “Reinforce the dehydrogenation process of LiAlH₄ by accumulating porous activated carbon,” *International Journal of Hydrogen Energy*, vol. 48, no. 43, pp. 16381–16391, May 2023, doi: 10.1016/j.ijhydene.2023.01.080.
- [47] Y. Qi, P. Sheng, H. Sun, J. Li, W. Zhang, S. Guo, D. Zhao, and Y. Zhang, “Hydrogen storage thermodynamics and kinetics of the as-cast and milled Ce-Mg-Ni-based alloy,” *Materials Today Communications*, vol. 35, Jun. 2023, Art. no. 106217, doi: 10.1016/j.mtcomm.2023.106217.



- [48] Y. Qi, P. Sheng, J. Li, X. Zhang, W. Zhang, S. Guo, and Y. Zhang, "Improved hydrogen storage thermodynamics and kinetics of La–Ce–Mg–Ni alloy by ball milling," *Journal of Physics and Chemistry of Solids*, vol. 179, Aug. 2023, Art. no. 111417, doi: 10.1016/j.jpms.2023.111417.
- [49] Y. Xu, Y. Zhou, Y. Li, and Z. Ding, "Carbon-based materials for Mg-based solid-state hydrogen storage strategies," *International Journal of Hydrogen Energy*, vol. 69, pp. 645–659, Jun. 2024, doi: 10.1016/j.ijhydene.2024.05.044.